

# Slabs of stabilized jellium: Quantum-size and self-compression effects

I. Sarria,<sup>1</sup> C. Henriques,<sup>2,3</sup> C. Fiolhais,<sup>3</sup> and J. M. Pitarke<sup>1,4</sup>

<sup>1</sup> *Materia Kondentsatuaren Fisika Saila, Zientzi Fakultatea, Euskal Herriko Unibertsitatea, 644 Posta kutxatila, 48080 Bilbo, Basque Country, Spain*

<sup>2</sup> *Departamento de Física, Faculdade de Ciências e Tecnologia, Universidade Nova de Lisboa, P-2825-114 Caparica, Portugal*

<sup>3</sup> *Center for Computational Physics, Department of Physics, University of Coimbra, P-3004-516 Coimbra, Portugal*

<sup>4</sup> *Donostia International Physics Center (DIPC) and Centro Mixto CSIC-UPV/EHU, Donostia, Basque Country, Spain*

(November 20, 2018)

We examine thin films of two simple metals (aluminum and lithium) in the stabilized jellium model, a modification of the regular jellium model in which a constant potential is added inside the metal to stabilize the system for a given background density. We investigate quantum-size effects on the surface energy and the work function. For a given film thickness we also evaluate the density yielding energy stability, which is found to be slightly higher than the equilibrium density of the bulk system and to approach this value in the limit of thick slabs. A comparison of our self-consistent calculations with the predictions of the liquid-drop model shows the validity of this model.

## I. INTRODUCTION

Thin films or slabs are systems made out of a few layers of atoms: they are finite in one direction and infinite in the other two perpendicular directions. Various theoretical models are available to calculate the electronic structure of slabs. One of the important features coming out of these calculations is the so-called quantum-size effect (QSE),<sup>1</sup> i.e., the influence of the finite size on various physical properties of the slab. These effects, which can be experimentally recognized,<sup>2</sup> decrease as the size of the slab increases. In fact, surface energies and work functions of the semi-infinite system are often derived from thin-slab calculations, which are simply extrapolated to this limit.<sup>3-6</sup>

The simplest model to predict the electronic structure of simple *sp*-bonded metals is the jellium model, where the ions are replaced by a positive neutralizing background. Within this model, the QSE of thin films was examined by Schulte.<sup>1</sup> He found an oscillatory behavior of the work function, as a function of the thickness of the slab. The same oscillatory behavior is found for the surface energy, defined as the energy required, per unit area of new surface formed, to split the solid in two along a plane.<sup>7</sup>

The jellium model has been referred to as giving insight into the realistic QSE appearing in real systems.<sup>8-10</sup> Notwithstanding important differences, an oscillatory pattern also appears in atomistic first-principles slab calculations of both the work function and the surface energy. Although the presence of the lattice may obscure the periodicity and the amplitude of the QSE, extrema were found at positions which agree with the jellium results. However, in the case of first-principles calculations difficulties arise (due to the cumbersome numerics) when one is to extract well-converged surface properties from

thin films made of typically 2 to 15 layers.<sup>5,6</sup> Hence, the clean jellium QSE, with no uncertainties in the extrapolated results, remains as a guide for more realistic investigations.

In this paper, we consider slabs in the framework of a simple modification of the jellium model which yields energy stability against changes in the background density. This so-called stabilized jellium<sup>11</sup> or structureless pseudopotential model yields realistic results, especially in the case of metals with high valence-electron density. For instance, the stabilized jellium model predicts positive surface energies that increase rapidly at high electron densities, as shown by experiment, while the jellium model predicts surface energies that are strongly negative at these densities. The stabilized jellium model, first introduced by Perdew, Tran, and Smith<sup>12</sup> and similar to the ideal-metal concept developed by Shore and Rose,<sup>13,14</sup> has been applied to the study of surfaces<sup>15,16</sup> and clusters.<sup>17</sup> In a way, the stabilized jellium is in between the jellium model and more sophisticated atomistic approaches: although it is still a continuous model (one may choose slabs with arbitrary thickness) with an analytical expression for the bulk energy, its physical predictions are in reasonable agreement with experiment. Besides including electrostatic corrections to the jellium model, the stabilized jellium model contains an averaged pseudopotential correction.

We calculate the self-consistent energetics (surface energy and work function) of slabs of stabilized jellium, with use of the local-density approximation (LDA) of density-functional theory (DFT).<sup>18,19</sup> We take two metals: Al ( $r_s = 2.07$ ,  $Z = 3$ ) and Li ( $r_s = 3.24$ ,  $Z = 1$ ), investigate the QSE, and compare our self-consistent slab calculations with those obtained for a semi-infinite stabilized jellium. We also test an extrapolation rule,<sup>20</sup> which has already been used to describe non-local surface ener-

gies of the bounded electron gas.<sup>21</sup>

Although the stabilized jellium model can be tailored to give face-dependent results,<sup>12,16,22</sup> it cannot describe the inhomogeneous relaxation predicted by first-principles calculations where the distances between atomic planes of the same family are optimized. However, an interesting effect displayed by the stabilized jellium model, which cannot be accounted for by the jellium model, is the so-called self-compression<sup>23</sup> (or self-expansion, in the case of charged systems<sup>24,25</sup>) of clusters. This effect, which can be classically viewed as the compression of a finite system due to the surface tension, is most prominent for small systems and almost negligible in the case of large clusters.

We investigate here the self-compression of thin films. We fix the size of the system along the direction perpendicular to the surface, and search for the background density which minimizes the total energy per valence electron of the slab. The equilibrium density is found to increase as the thickness of the slab decreases, and to converge to the bulk electron density in the infinite-thickness limit. Furthermore, the equilibrium electron-density parameter  $r_s^*$  is found to oscillate with the slab thickness, as a manifestation of the QSE, but the general trend is found to be well described within the liquid-drop model (LDM)<sup>26,27</sup> based only on the knowledge of the bulk energy per unit volume and the surface energy. We discuss the relationship between this self-compression effect and the relaxation of metal slabs predicted by atomistic first-principles calculations.

In section II we present briefly the stabilized jellium model for slabs. In section III we discuss the results we obtained within this model. The main conclusions are drawn in section IV, where further comments on the relationship between the stabilized jellium and more elaborated models are made. Equations are written in atomic units throughout, i.e.,  $e^2 = \hbar = m_e = 1$ .

## II. SLABS OF STABILIZED JELLIUM

The stabilized jellium model<sup>12</sup> takes into account the lattice ions, but keeps the essential simplicity of the jellium model. The total energy is obtained as a functional of the electron density  $n(\mathbf{r})$ , in the following way:

$$E_{SJ}[n, n_+] = E_J[n, n_+] + (e_M + \bar{w}_R) \int d^3r n_+(\mathbf{r}) + \langle \delta v \rangle_{WS} \int d^3r \frac{n_+(\mathbf{r})}{\bar{n}} [n(\mathbf{r}) - n_+(\mathbf{r})], \quad (1)$$

where

$$n_+ = \bar{n} \Theta(\mathbf{r}) \quad (2)$$

represents a positive neutralizing background density,  $\Theta(\mathbf{r})$  being a function which equals 1 inside a given surface and 0 outside, and

$$\bar{n} = \frac{3}{4\pi r_s^3} \quad (3)$$

is the average valence-electron density.  $E_J$  is the regular-jellium total energy,  $e_M$  is the Madelung energy arising from the Coulomb interaction between a uniform negative background inside the spherical Wigner-Seitz cell and a point ion at its center,

$$e_M = -\frac{9Z^{2/3}}{10r_s}, \quad (4)$$

$\bar{w}_R$  is the average value of the repulsive non-Coulomb part of the Ashcroft empty-core pseudopotential,

$$\bar{w}_R = 2\pi\bar{n}r_c^2, \quad (5)$$

and  $\langle \delta v \rangle_{WS}$  represents the difference between the local pseudopotential and the jellium potential, averaged over the Wigner-Seitz cell,

$$\langle \delta v \rangle_{WS} = \frac{3r_c^2}{2r_s^3} - \frac{3Z^{2/3}}{10r_s}. \quad (6)$$

The core radius  $r_c$  of the Ashcroft empty-core pseudopotential is chosen to stabilize the metal for given values of the electron-density parameter  $r_s$  and the chemical valence  $Z$ .

The two terms added to the regular-jellium energy  $E_J$  are a volume term and a surface term. They simply account for the subtraction of the spurious self-interaction of the positive jellium background and the inclusion of a constant structureless potential inside the metal. This procedure may be understood as a first-order perturbation to a jellium system, but with the perturbation treated in an averaged manner.

The density functional of Eq. (1) represents the total energy of an arbitrary inhomogeneous system. In the case of an infinite uniform system, the equilibrium density is obtained from the bulk stability condition

$$\frac{d\epsilon_{SJ}^{bulk}}{dr_s} = 0, \quad (7)$$

where

$$\epsilon_{SJ}^{bulk} = e_J^{bulk} + e_M + \bar{w}_R \quad (8)$$

represents the average bulk energy per valence electron,  $e_J$  being the regular-jellium contribution. Within this model any individual metal minimizes the energy at a given equilibrium density, while the jellium energy presents a single minimum at  $r_s \sim 4.2$  close to the electron-density parameter of sodium.

We consider slabs of stabilized jellium. Slabs are translationally invariant in the plane of the surface, which is assumed to be perpendicular to the  $z$  axis. Hence, the single-particle wave functions can be separated into a plane wave along the surface and a component  $\phi(z)$  describing motion normal to the surface with energy  $\epsilon$ .

This component is obtained by solving self-consistently the Kohn-Sham equation

$$\left[ -\frac{1}{2} \frac{d^2}{dz^2} + V_H(z) + V_{xc}(z) + V_{ps}(z) \right] \phi(z) = \epsilon \phi(z), \quad (9)$$

where  $V_H(z)$  represents the Hartree electrostatic potential,  $V_{xc}(z)$  is the exchange-correlation potential, and  $V_{ps}(z)$  accounts for the pseudopotential,

$$V_{ps}(z) = \langle \delta v \rangle_{WS} \Theta(z). \quad (10)$$

$V_{xc}(z)$  is obtained in the LDA, using the electron-gas correlation energy of Ceperley and Alder,<sup>28</sup> as parameterized by Perdew and Wang,<sup>29</sup> Essentially the same results are obtained from the parameterizations of Vosko, Wilk, and Nusair<sup>30</sup> and of Perdew and Zunger.<sup>31</sup> We have not chosen to use extensions such as the generalized gradient approximation (GGA),<sup>32</sup> since the LDA has been shown to give surprisingly good results in describing the properties of jellium planar surfaces.<sup>33</sup>

Outside the positive background the electron-density profile  $n(z)$  decays rapidly from its bulk value  $\bar{n}$ . The electronic system can therefore be taken to be finite in the  $z$  direction by assuming that  $n(z)$  actually vanishes at a given distance  $z_0$  from the surface. Hence, we introduce infinite potential walls at a distance  $z_0$  from each surface, and follow Ref. 34 to expand the wave functions  $\phi(z)$  in a Fourier sine series. The distance  $z_0$  (typically 2 or 3 Fermi wavelengths) and the number of sines kept in the expansion of the wave functions  $\phi(z)$  have been chosen to be sufficiently large for our calculations to be insensitive to the precise values employed. These calculations have been compared with others which we have carried out for a semi-infinite electron system by using the Monnier-Perdew code<sup>35</sup> for the numerical integration of Eq. (9).

For a given thickness  $L$  of the slab, we obtain the surface energy from the difference between the total energy of Eq. (1) and the corresponding result for a homogeneous electron gas of density  $n_+$ , i.e.,

$$\sigma(L) = \frac{1}{2A} [E_{SJ}(L) - \bar{n} L A \epsilon_{SJ}^{bulk}], \quad (11)$$

where  $A$  is the normalization area. The work function is obtained as the difference between the computed values for the vacuum and Fermi levels of our electron system.

### III. RESULTS AND DISCUSSION

First of all, we compare jellium and stabilized-jellium electron densities  $n(z)$  and effective potentials,

$$V_{eff}(z) = V_H(z) + V_{xc}(z) + V_{ps}(z). \quad (12)$$

Jellium and stabilized-jellium valence-electron densities and effective potentials for an Al slab of  $L = 2 \lambda_F$  [ $\lambda_F = (32 \pi^2/9)^{1/3} r_s$  is the Fermi wavelength] are shown

in Fig. 1, together with the positive background density  $n_+$ . We note that the stabilized-jellium electron density is steeper at the two surfaces, so that the electronic spill-out is slightly smaller within this model. This is due to the fact that electrons feel a deeper effective potential. Both jellium and stabilized-jellium electron densities exhibit quantum oscillations inside the metal, the so-called Friedel oscillations,<sup>7</sup> and an exponential decay outside.

Figs. 2 and 3 show our calculated stabilized-jellium surface energies for slabs of Al and Li, respectively, as obtained from Eq. (11) versus the thickness  $L$  of the slab. Both curves show damped oscillations with minima occurring at the slab width  $L \sim n \lambda_F/2$  ( $n = 1, 2, \dots$ ). The same QSE, which reflects the quantization of the electronic motion along one direction, is known to occur within the jellium model.<sup>1</sup>

Both the average bulk energy per valence electron  $\epsilon_{SJ}^{bulk}$  and the surface energy of the semi-infinite stabilized jellium

$$\sigma = \lim_{L \rightarrow \infty} \sigma(L) \quad (13)$$

may be obtained from a linear fit of the following equation:

$$\frac{E_{SJ}(L)}{A} = 2\sigma + \bar{n} L \epsilon_{SJ}^{bulk}, \quad (14)$$

where  $E_{SJ}(L)$  represents the total energy of Eq. (1). Following this procedure, we reproduce the bulk energy of Eq. (8) and predict surface energies of 925 erg/cm<sup>2</sup> and 311 erg/cm<sup>2</sup> for Al and Li, respectively. These surface energies, represented in Figs. 2 and 3 by horizontal solid lines, agree with those reported in Ref. 16 for semi-infinite media.

An alternative procedure to extrapolate the surface energy  $\sigma$  of the semi-infinite medium from our calculated thin-film surface energies  $\sigma(L)$  is to use the relation<sup>20</sup>

$$\sigma = \frac{\sigma(L_n - \lambda_F/4) + \sigma(L_n) + \sigma(L_n + \lambda_F/4)}{3}, \quad (15)$$

where  $L_n$  represents the threshold width for which the  $n$ th subband for the  $z$  motion is first occupied. Analytical insight for this procedure is encountered within the infinite-barrier model (IBM), where the effective potential  $V_{eff}(z)$  is replaced by an infinite square well and the one-particle wave functions  $\phi(z)$  are simply sines. Based on this procedure, the numerical error introduced in  $\sigma$  by our slab calculations is found to be within 0.1%. The advantage of this algorithm is that we simply need three points to obtain the asymptotic limit, while the linear fitting may yield erroneous results if one only takes a few thin films.

Slabs with  $L < 0.5 \lambda_F$  are interesting in their own, since they can be constructed in the laboratory, e.g., by joining two different semiconductors. Nevertheless, we do not give results for these ultra-thin slabs, since they

fall within the two-dimensional limit where the three-dimensional LDA and GGA formulae for exchange and correlation are known to fail.<sup>36</sup>

For comparison, first-principles thin-film calculations of the surface energy of the most dense faces of Al and Li [(111) for fcc Al and (0001) for hcp Li] are represented in Figs. 2 and 3 by solid circles and triangles, with the slab width of a  $\nu$ -layer unrelaxed crystalline film taken to be  $\nu$  times the interplanar distance. For Al there is reasonable agreement between our stabilized-jellium results and atomistic first-principles calculations, the amplitude of the stabilized-jellium oscillations being comparable to that exhibited by first-principles calculations. For Li, however, there is a serious discrepancy between stabilized-jellium and first-principles calculations. Since lithium has been found to behave to some extent like a covalent solid rather than a free-electron gas,<sup>37–40</sup> it is not expected to be well described by a jellium-like model.

A face-dependent approach extension of the stabilized-jellium model consists in obtaining the self-consistent electron density by adding to the constant potential  $\langle\delta v\rangle_{WS}$  a structure-dependent corrugation factor.<sup>12,16</sup> This procedure yields an increased surface energy [horizontal dashed-dotted lines of Figs. 2 and 3], which in the case of Al is found to be close to the experimental result.

Figs. 4 and 5 exhibit our calculated stabilized-jellium work functions for slabs of Al and Li, respectively, as a function of the thickness  $L$  of the slab, together with first-principles thin-film calculations. As in the case of the surface energy, a procedure similar to that of Eq. (15) yields a work function [represented by horizontal solid lines] that agrees within less than 0.1% with the result we also obtain after solving Eq. (9) for the semi-infinite medium, a precision that is difficult to achieve by a fitting procedure. For  $L \sim 0.5\lambda_F$ , the QSE yields oscillations with relative amplitudes of  $\sim 20\%$  and  $\sim 10\%$  for Al and Li, respectively. For Al both the amplitude and the oscillation pattern are comparable to those exhibited by atomistic calculations. In the case of a 3-layer film of Al(111), the slab width is  $L \sim 4(\lambda_F/2)$ . Hence, the stabilized-jellium model predicts a minimum for this film, which is in reasonable agreement with the deep minimum exhibited by atomistic calculations with  $\nu = 3$ . In the case of Li(0001), the stabilized-jellium model predicts a minimum for a one-layer film [ $L \sim 1(\lambda_F/2)$ ], also in agreement with the minimum exhibited by first-principles calculations with  $\nu = 1$ . Finally, we note that adding a structure-dependent corrugation factor to the stabilized-jellium  $\langle\delta v\rangle_{WS}$  constant potential yields a smaller value of the work function [horizontal dashed-dotted lines of Figs. 4 and 5], which in the case of Al is in reasonable agreement with the experiment. For Li, both the stabilized-jellium model and first-principles calculations predict work functions that are well above the experimental result.

For given values of the equilibrium-density parameter  $r_s$  and the valence  $Z$ , all these calculations have been carried out with the core radius  $r_c$  [characteristic of each

metal] that is obtained from the bulk stability condition expressed by Eq. (7). However, while at the equilibrium density  $\bar{n}$  of Eq. (3) the infinite homogeneous system is stable, at this density a finite system is not stable against changes of the background density, i.e.,

$$\frac{d(E/N)}{dr_s} \neq 0, \quad (16)$$

where  $N$  represents the particle number. Instead, there is a modified equilibrium-density parameter  $r_s^*$ , which stabilizes the finite system. This modified parameter depends on the size  $L$  of our system and is expected to approach  $r_s$  as  $L \rightarrow \infty$ .

Fig. 6 shows the result of our full self-consistent Kohn-Sham calculations of the deviation  $r_s^* - r_s$ , as a function of the thickness  $L$  of the slab. These calculations indicate that there is a self-compression effect, which is more pronounced when the two surfaces are separated by a multiple of  $\sim \lambda_F/2$ .

The self-compression effect exhibited in Fig. 6 may be approximately predicted with use of the LDM, a simple model to evaluate the total energy of a finite system.<sup>26,27</sup> In this model, the energy is the sum of a volume term (the bulk energy per unit volume,  $\bar{n}\epsilon_{bulk}$ , times the volume) and a surface term (the surface energy,  $\sigma$ , times the transversal area):

$$E_{LDM} = \bar{n}\epsilon_{bulk}V + \sigma A. \quad (17)$$

For fixed  $r_c$ , and evaluated at the *bulk* equilibrium-density parameter  $r_s$ ,

$$\frac{d(E_{LDM}/N)}{dr_s} = \frac{A}{N} \frac{d\sigma}{dr_s} + \sigma \frac{d(A/N)}{dr_s} > 0. \quad (18)$$

The first term is positive, as can be found from the data in Table I of Ref. 23. For a fixed slab width  $L$ , the second term is also positive, and the surface term self-compresses, therefore, stabilized-jellium slabs. The deviation of the electron density parameter  $r_s^*$  obtained from the LDM stability condition

$$\frac{d(E_{LDM}/N)}{dr_s} = 0 \quad (19)$$

with respect to the *bulk* equilibrium density parameter  $r_s$  is also plotted in Fig. 6, showing that the LDM provides a nice average of our self-consistent Kohn-Sham calculations, as previously demonstrated in the case of clusters.<sup>23</sup>

In Ref. 9, thin films of Be with 1-3 layers were examined and a jellium version of a crystalline calculation was considered. The electron density parameter  $r_s^*$  needed to define each slab was derived from the optimized (relaxed) structural parameters. The results reported in Ref. 9 are in agreement with the compression effect we report here, with  $r_s^*$  increasing with the number of layers and approaching the *bulk* equilibrium-density parameter  $r_s$  as

$L \rightarrow \infty$ . These results show deviations of the electron density parameter,  $r_s^* - r_s$  of  $\sim 3.2\%$ ,  $1.9\%$  and  $0.9\%$  for thin films with 1, 2 and 3 layers, respectively. This is in agreement with our stabilized-jellium calculations, which in the case of thin films with  $\sim 2$  layers of Li and Al predict (see Fig. 6) differences between  $r_s^*$  and  $r_s$  of  $\sim 1.6\%$  and  $1.8\%$ , respectively. The self-compression of structural parameters in ultra-thin crystalline films has also been discussed in terms of the so-called coordination model which, however, seems to fail in some cases (see, e.g., Ref. 41).

Finally, we note that if for each value of  $L$  the corresponding equilibrium-density parameter  $r_s^*$  is taken, instead of the *bulk* parameter  $r_s$ , modified surface energies and work functions are obtained which are quite similar to those displayed in Figs. 2-5. This is in contrast with the discussion of Ref. 9.

#### IV. CONCLUSIONS

We have modeled thin films of two simple metals, aluminum and lithium, using the stabilized-jellium model, and have studied the convergence of some physical quantities (work function and surface energy) to the semi-infinite planar-surface results. We have found the same oscillatory behavior which is typical of the QSE in jellium. Although this behavior also shows up in atomistic first-principles thin-film calculations, the clean QSE of continuous background models is obscured in the more realistic calculations. A trend consisting in surface energy minima coinciding with work function maxima was reported for first-principles crystalline calculations.<sup>42,43</sup> However, within the stabilized-jellium model we have found minima and maxima of both quantities at the same positions [as also reported in Ref. 4 from first-principles for Al(111)]. On the other hand, we have found that both the absolute and the relative amplitude of stabilized-jellium QSE oscillations are larger for aluminum than for lithium, in agreement with first-principles evaluations. The disagreement between our stabilized-jellium results for lithium and the more realistic atomistic *all-electron* calculations cannot be attributed to some property of the pseudopotential, and simply shows that this metal does not display free-electron behaviour.

Stabilized-jellium slabs of aluminum and lithium have been found not to be stable at the *bulk* equilibrium density, the size-dependent equilibrium density being larger. This self-compression effect, which was already known to exist for clusters, has been found to become more important as the slab width decreases. Both LDM and full self-consistent DFT calculations have shown a larger self-compression for aluminum than for lithium, which is a consequence of the larger surface energy of the former material. The self-compression of thin simple-metal films is a general rule that is also exhibited by atomistic first-principles calculations, where the unitary cell of thin

films is found to be slightly smaller than that of the bulk solid.

The stabilized jellium model is computationally as simple as the jellium model; however, for the two high-density metals we have considered, it is much more realistic. In particular, we have found it to be more realistic for aluminum than for lithium. The stabilized-jellium model is adequate to obtain general qualitative conclusions and an understanding of trends of simple metals but, obviously, is unable to provide precise quantitative conclusions on particular metals. These can only be extracted from the now standard first-principles, but computationally more demanding, calculations.

#### V. ACKNOWLEDGMENTS

The authors gratefully acknowledge J. P. Perdew for fruitful discussions. This project has been supported by the University of the Basque Country, the Basque Hezkuntza, Unibertsitate eta Ikerketa Saila, the Spanish Ministerio de Educación y Cultura, and the Portuguese PRAXIS XXI Program (Project PRAXIS/2/2.1/FIS/473/94).

- 
- <sup>1</sup> F. K. Schulte, Surf. Sci. **55**, 427 (1976).
  - <sup>2</sup> R. C. Jaklevic and J. Lambe, Phys. Rev. B **12**, 4146 (1975).
  - <sup>3</sup> J. C. Boettger, Phys. Rev. B **49**, 16798 (1994).
  - <sup>4</sup> J. C. Boettger, Phys. Rev. B **53**, 13133 (1996).
  - <sup>5</sup> V. Fiorentini and M. Methfessel, J. Phys.: Condens. Mat. **8**, 6525 (1996).
  - <sup>6</sup> J. C. Boettger, J.R. Smith, U. Birkenheuer, N. Rösch, S. B. Trickey, J. R. Sabin, and S. P. Apell, J. Phys.: Condens. Mat. **10**, 893 (1998).
  - <sup>7</sup> See, e.g., N. D. Lang, Solid State Phys. **28**, 225 (1973).
  - <sup>8</sup> P.J. Feibelman, Phys. Rev. B **27**, 1991 (1983).
  - <sup>9</sup> J. L. Vicente, A. Paola, A. Razzitte, E. E. Mola, and S. B. Trickey, Phys. Stat. Sol. B **155**, K93 (1989).
  - <sup>10</sup> K. F. Wojciechowski and H. Bogdanow, Surf. Sci. **397**, 53 (1998).
  - <sup>11</sup> A. Kiejna, Prog. Surf. Sci. **61**, 65 (1999).
  - <sup>12</sup> J. P. Perdew, H. Q. Tran, and E. D. Smith, Phys. Rev. B **42**, 11627 (1990).
  - <sup>13</sup> H. B. Shore and J. H. Rose, Phys. Rev. Lett. **66**, 2519 (1991); J. H. Rose and H. B. Shore, Phys. Rev. B **43**, 11605 (1991).
  - <sup>14</sup> H. B. Shore and J. H. Rose, Phys. Rev. B **59**, 10485 (1999).
  - <sup>15</sup> C. Fiolhais and J. P. Perdew, Phys. Rev. B **45**, 6207 (1992).
  - <sup>16</sup> A. Kiejna, Phys. Rev. B **47**, 7361 (1993). Small differences between surface energies reported in Ref. 15 and those of this reference are due to improved numerics in the later.
  - <sup>17</sup> M. Brajczewska, C. Fiolhais, and J. P. Perdew, Int. J. Quantum Chem. **27**, 249 (1993).

- <sup>18</sup> P. Hohenberg and W. Kohn, Phys. Rev. **136**, B864 (1964); W. Kohn and L. J. Sham, Phys. Rev. **140**, A11333 (1965).
- <sup>19</sup> R. M. Dreizler and E. K. U. Gross, *Density Functional Theory* (Springer-Verlag, Berlin, 1990).
- <sup>20</sup> J. M. Pitarke and A. G. Eguiluz (unpublished).
- <sup>21</sup> J. M. Pitarke and A. G. Eguiluz, Phys. Rev. B **57**, 6329 (1998).
- <sup>22</sup> J. P. Perdew, Progr. Surf. Sci. **48**, 795 (1995).
- <sup>23</sup> J. P. Perdew, M. Brajczewska, and C. Fiolhais, Sol. Stat. Com. **88**, 795 (1993).
- <sup>24</sup> A. Vieira, M. Brajczewska, C. Fiolhais, and J. P. Perdew, Int. J. of Quantum Chem. **60**, 1537 (1996).
- <sup>25</sup> M. Brajczewska, A. Vieira, C. Fiolhais, and J. P. Perdew, Prog. Surf. Sci. **53**, 315 (1996).
- <sup>26</sup> W. D. Myers and W. J. Swiatecki, Ann. Phys. (N. Y.) **55**, 395 (1969); **84**, 186 (1974).
- <sup>27</sup> J. P. Perdew, Y. Wang, and E. Engel, Phys. Rev. Lett. **66**, 508 (1991).
- <sup>28</sup> D. M. Ceperley and B. J. Alder, Phys. Rev. Lett. **45**, 1196 (1980).
- <sup>29</sup> J. P. Perdew and Y. Wang, Phys. Rev. B **45**, 13244 (1992).
- <sup>30</sup> H. Vosko, L. Wilk, and M. Nusair, Can. J. Phys. **58**, 1200 (1980).
- <sup>31</sup> J. P. Perdew and A. Zunger, Phys. Rev. B **23**, 5048 (1981).
- <sup>32</sup> J. P. Perdew, K. Burke, and M. Ernzerhof, Phys. Rev. Lett. **77**, 3865 (1996).
- <sup>33</sup> S. Kurth and J. P. Perdew, Phys. Rev. B **59**, 10461 (1999); Z. Yan, J. P. Perdew, S. Kurth, C. Fiolhais, and L. Almeida, Phys. Rev. B **61**, 2595 (2000).
- <sup>34</sup> A. G. Eguiluz, D. A. Campbell, A. A. Maradudin, and R. F. Wallis, Phys. Rev. B **30**, 5449 (1984); A. G. Eguiluz, Phys. Scr. **36**, 651 (1987).
- <sup>35</sup> R. Monnier and J. P. Perdew, Phys. Rev. B **17**, 2595 (1978).
- <sup>36</sup> L. Pollack and J. P. Perdew, J. Phys.: Condens. Mat. **12**, 1241 (2000).
- <sup>37</sup> K. Doll, N. M. Harrison, and V. R. Saunders, J. Phys.: Condens. Mat. **11**, 5007 (1999).
- <sup>38</sup> J. C. Boettger and S. B. Trickey, Phys. Rev. B **45**, 1363 (1992).
- <sup>39</sup> U. Birkenheuer, J.C. Boettger, and N. Rösch, Surf. Sci. **341**, 103 (1995).
- <sup>40</sup> K. Kokko, P.T. Salo, R. Laihia, K. Mansikka, Surf. Sci. **348**, 168 (1996).
- <sup>41</sup> J. C. Boettger, S. B. Trickey, F. Muller-Plathe, G. H. F. Dierksen, J. Phys.: Condens. Mat. **2**, 9589 (1990).
- <sup>42</sup> I. P. Batra, S. Ciraci, G. P. Srivastava, J. S. Nelson, and C. Y. Fong, Phys. Rev. B **34**, 8246 (1986).
- <sup>43</sup> A. Kiejna, J. Peisert, and P. Scharoch, Surf. Sci. **432**, 54 (1999).
- <sup>44</sup> W. R. Tyson and W. A. Miller, Surf. Sci. **62**, 267 (1977).
- <sup>45</sup> P. J. Feibelman and D. R. Hamann, Phys. Rev. B **29**, 6463 (1984).
- <sup>46</sup> H. B. Michaelson, J. Appl. Phys. **48**, 4729 (1997).

FIG. 1. Normalized valence-electron density in the jellium model (solid line) and in the stabilized-jellium model (dashed line) for a slab of Al ( $r_s = 2.07$ ) with thickness  $L = 2 \lambda_F$ . The background density is represented by the dark area. The figure also displays the effective potential  $V_{eff}(z)$  in each model (solid line for the jellium model and dashed line for the stabilized-jellium model).

FIG. 2. Surface energy and QSE in aluminum ( $r_s = 2.07$ ). Large vertical marks across the horizontal axis show the widths of unrelaxed fcc Al(111) slabs with  $\nu = 1, \dots, 12$  atomic planes. The width  $L$  is given by  $L = \nu(\sqrt{3}/3)a$ ,  $a$  being the lattice parameter  $a = (16\pi Z/3)^{1/3}r_s$ . The solid oscillating line shows our calculated surface energy of flat stabilized-jellium slabs. Solid and dashed-dotted horizontal lines represent our calculated surface energy of semi-infinite flat Al (solid line) and fcc Al(111) (dashed-dotted line) stabilized jellia. The zero-temperature extrapolation of the experimental liquid-metal surface tension of Ref. 44 divided by 1.2,<sup>27</sup> is represented by an horizontal arrow. For comparison, atomistic first-principles calculations from Refs. 42 and 4 are also displayed, by solid circles and triangles, respectively. The surface energies of Ref. 42 were obtained using the self-consistent pseudopotential method combined with an independent calculation of the bulk energy per electron. The surface energies of Ref. 4 were obtained within an all-electron scheme with the use of a linear-combination-of-gaussian-type-orbitals fitting function (LCGTO-FF) and with the bulk energy per electron extracted from the slab calculations. Dashed lines are to guide the eye.

FIG. 3. Surface energy and QSE in lithium ( $r_s = 3.24$ ). Large vertical marks across the horizontal axis show the widths of unrelaxed hcp Li(0001) slabs with  $\nu = 1, \dots, 12$  atomic planes [ $c/a = 1.64^{38}$ , which corresponds to  $r_s = 3.13$ ]. The slab width is  $L = \nu a/2$  and the structural-parameters' ratio  $c/a = (16\sqrt{3}\pi Z/9)(r_s/a)^3$ . The solid oscillating line shows our calculated surface energy of flat stabilized-jellium slabs. Solid and dashed-dotted horizontal lines represent our calculated surface energy of semi-infinite flat Li (solid line) an hcp Li(0001) (dashed-dotted line) stabilized jellia. The horizontal arrow has the same meaning as in Fig. 2. For comparison, atomistic all-electron calculations from Refs. 38 and 39 are also displayed, by solid circles. These surface energies were obtained with the use of a LCGTO-FF and with the bulk energy per electron extracted from the slab calculations. Dashed lines are to guide the eye.

FIG. 4. Work function and QSE in aluminum ( $r_s = 2.07$ ). All symbols have the same meaning as in Fig. 2. For comparison, atomistic all-electron calculations from Refs. 8 and 45 are also displayed, by solid squares and rhombs, respectively. The work functions of Ref. 8 were obtained within the LCAO scheme, and those of Ref. 45 were obtained with the use of surface linearized augmented plane waves (SLAPW). The experimental polycrystalline work function of Ref. 46 is represented by an horizontal arrow.

FIG. 5. Work function and QSE in lithium ( $r_s = 3.24$ ). All symbols have the same meaning as in Fig. 3. The experimental polycrystalline work function of Ref. 46 is represented by an horizontal arrow.

FIG. 6. Relative difference between the actual equilibrium-density parameter  $r_s^*$  and the *bulk* density parameter  $r_s$  for aluminum (dashed lines) and lithium (solid lines) stabilized-jellium films, as a function of the slab width  $L$ .

Fig. 1

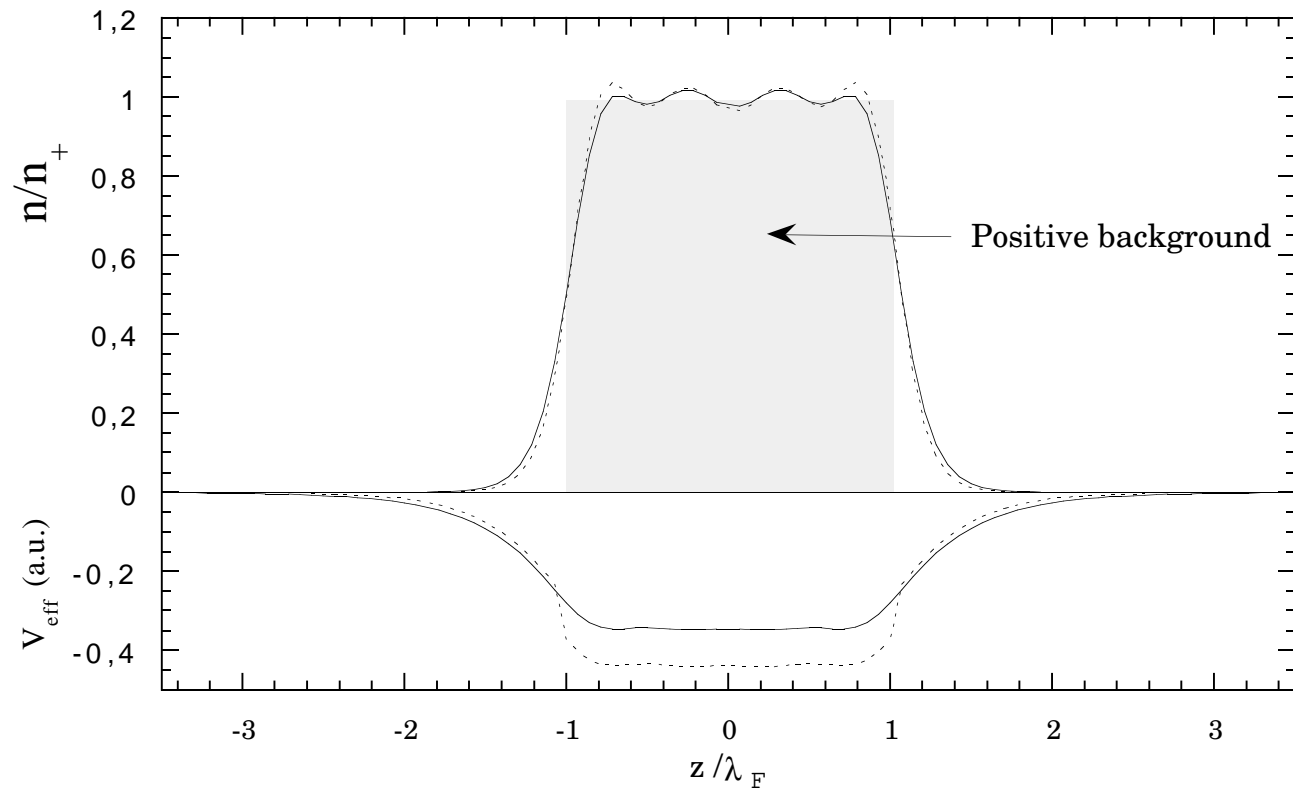




Fig. 2

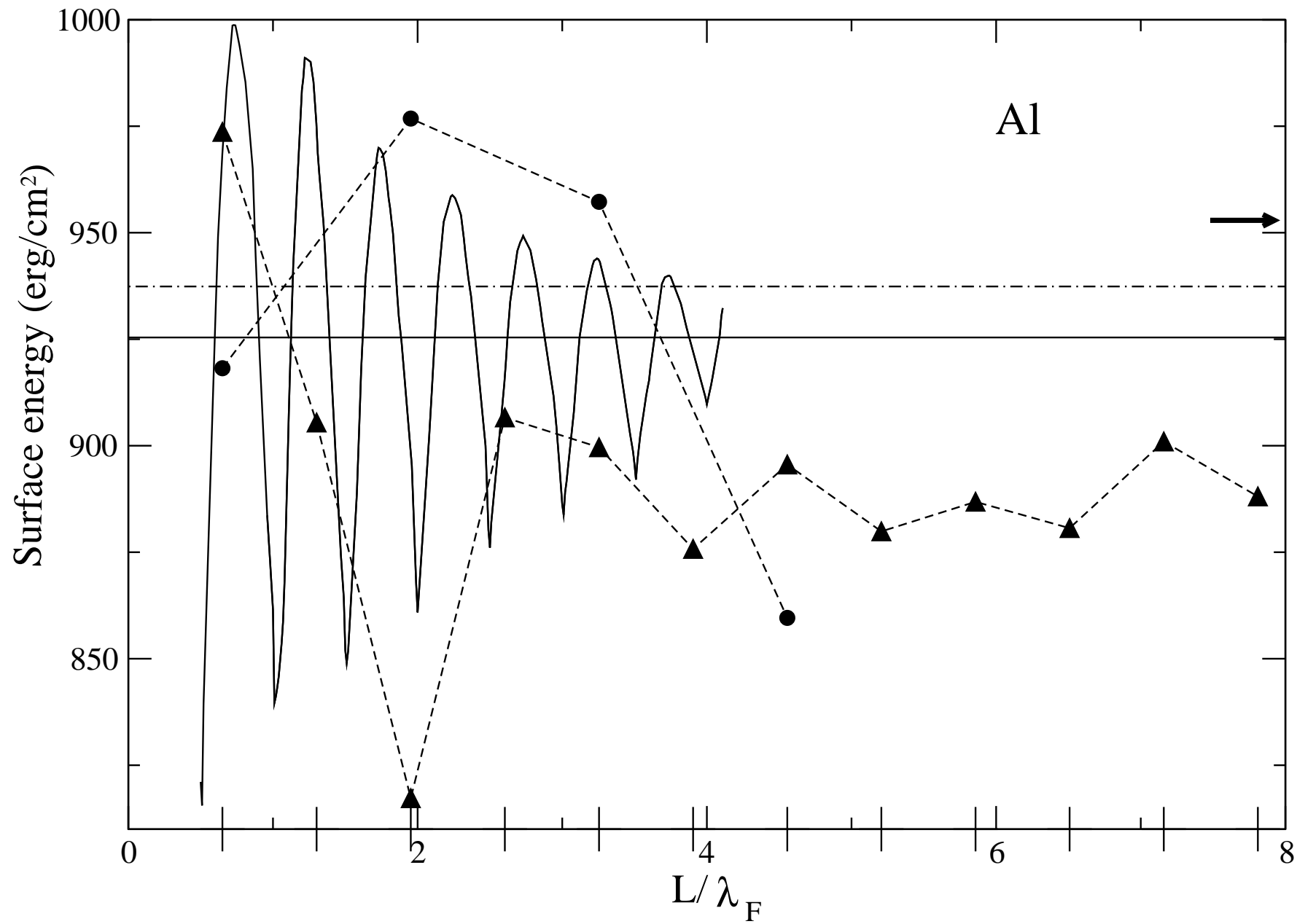


Fig. 3

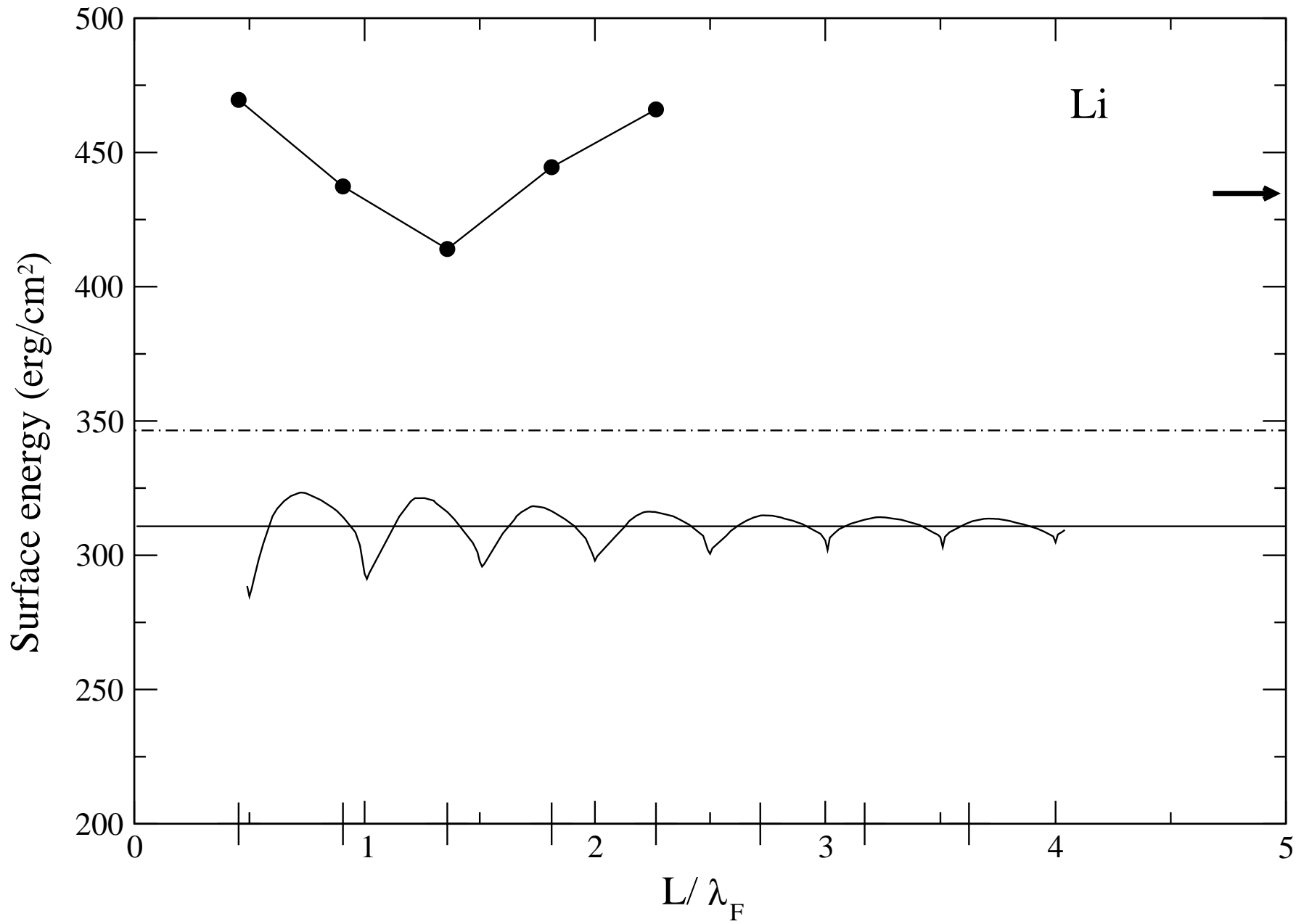


Fig. 4

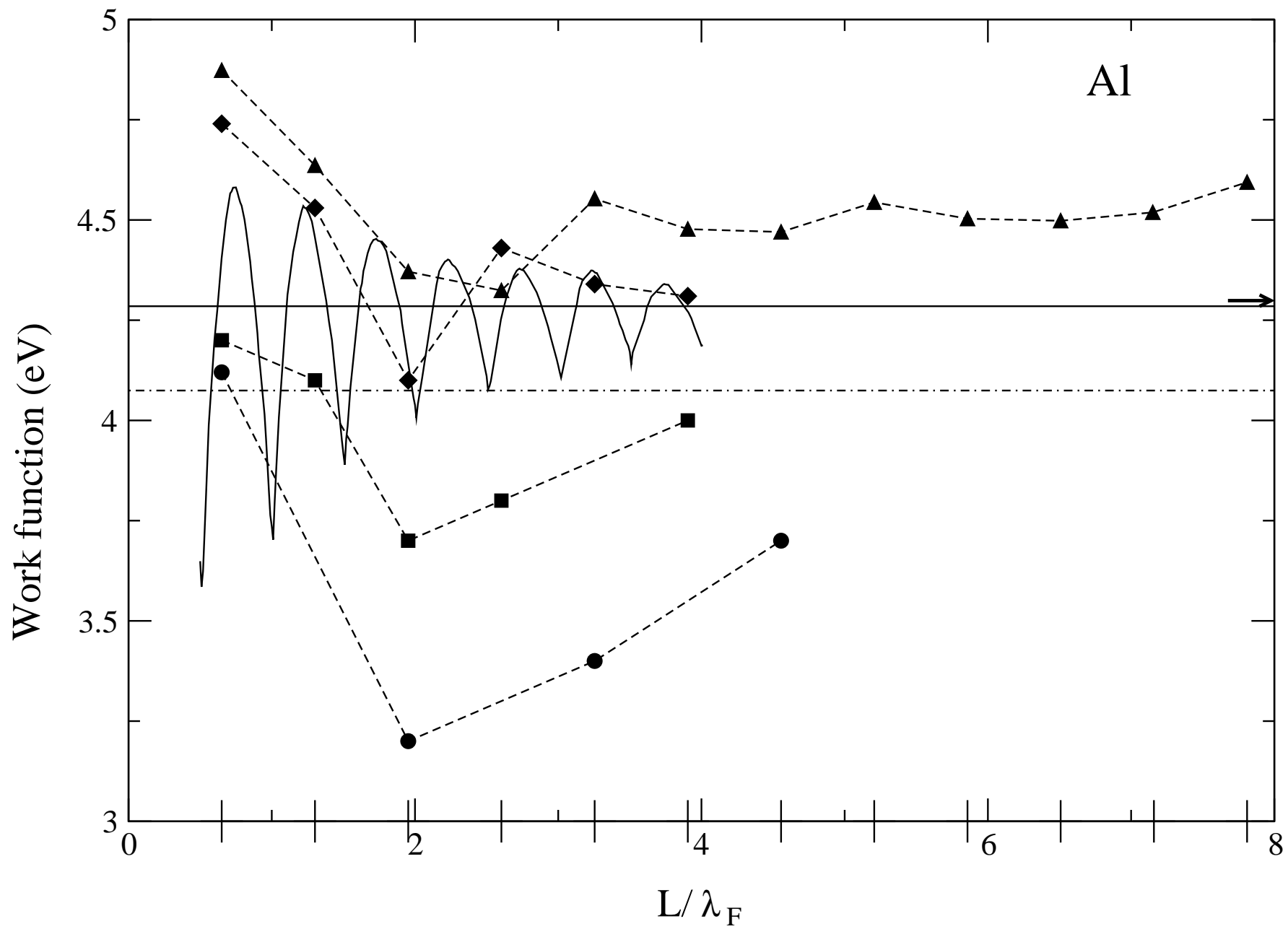


Fig. 5

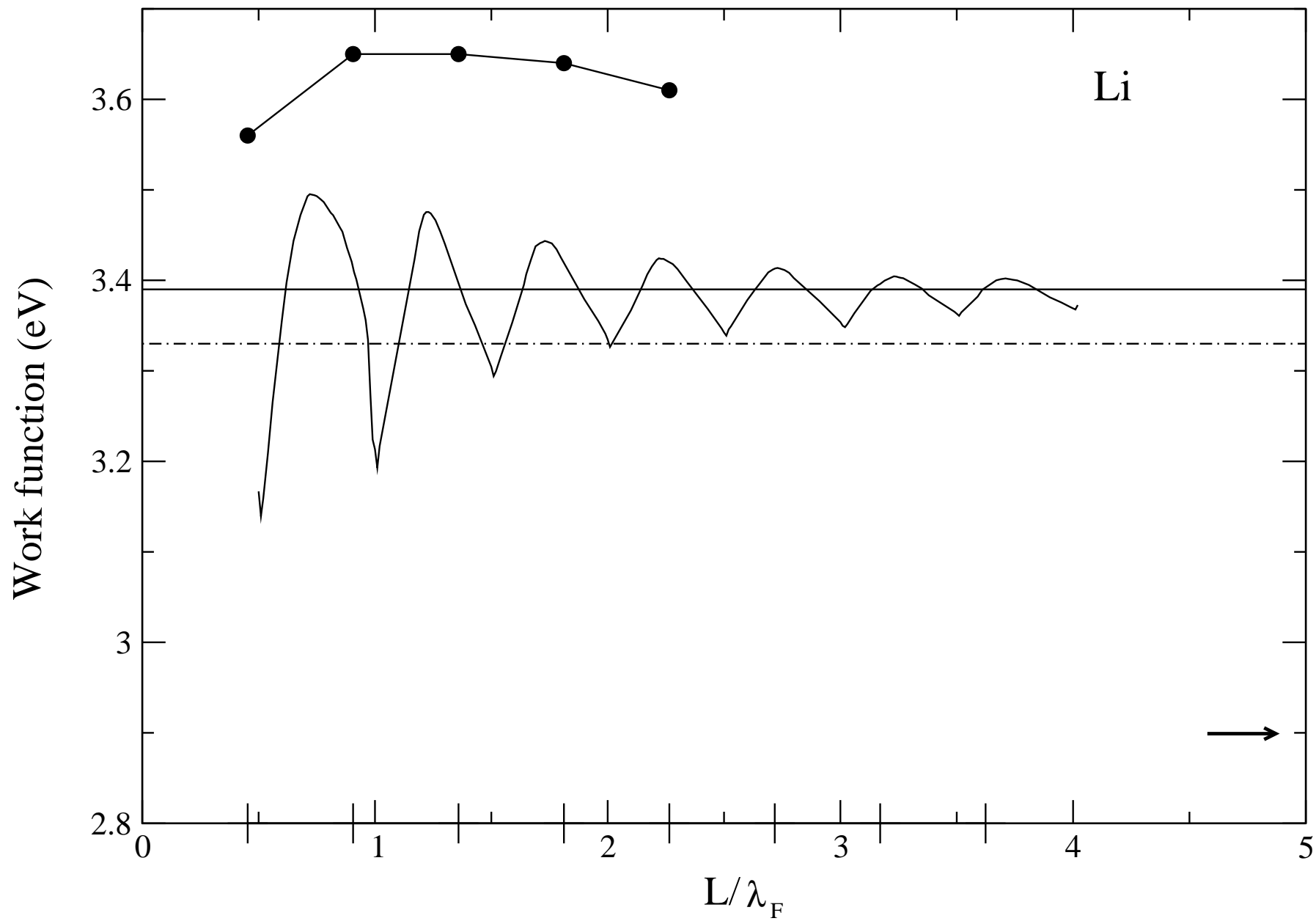


Fig. 6

